$T_{cc}(3875)^+$ with different quark masses

Michael Abolnikov

Institute of Theoretical Physics II, Ruhr University Bochum

September 2024

Annual meeting of the German LHCb groups

talk based on 2407.04649v1 (2024)

in collaboration with

V. Baru, E. Epelbaum, A. Filin, C. Hanhart, L. Meng

Introduction

LHCb Collaboration 2022

T_{cc}^{+}: $cc\bar{u}\bar{d}$ exotic candidate, $\delta m = (-360 \pm 40)$ keV, $\Gamma_{\text{pole}} = (48 \pm 2)$ keV and $I = 0$, $J^P = 1^+$

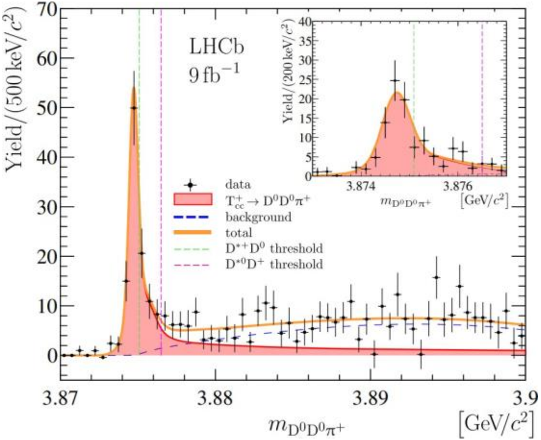

Introduction - Contribution of the width to the pole

T_{cc}^{+} lies right below the $D^0 D^{*+}$ threshold but is also close to the $D^+ D^{*0}$ threshold. It can decay to three-body channels due to the D^* width:

$$T_{cc}^{+} \to D^0 D^{*+} \to D^0 D^0 \pi^+ / D^0 D^+ \pi^0$$
$$T_{cc}^{+} \to D^+ D^{*0} \to D^+ D^0 \pi^0 / D^+ D^0 \gamma$$

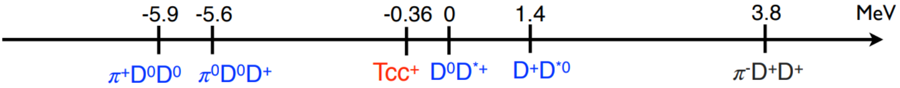

→ Correction of the full width to $\Gamma_{\text{pole}} = (56 \pm 2)$ keV by explicitly including three-body $(DD\pi)$ dynamics Du et al. 2022

Introduction - Beyond the physical point

Lattice studies provide insights on the properties of T_{cc}^+ beyond physical quark masses. Some examples are

- $E_{\text{pole}} = -9.9^{+3.6}_{-7.2}$ MeV, **virtual state** at $m_\pi = 280$ MeV
  Padmanath, Prelovsek 2022

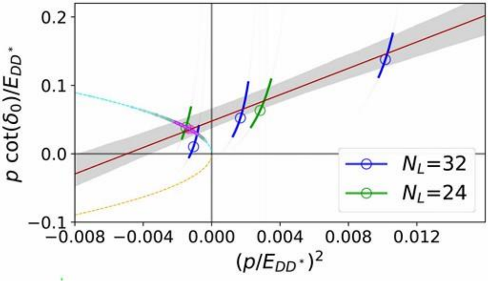

- $E_{\text{pole}} = -59^{+53}_{-99}$ keV, **virtual state** at $m_\pi = 146$ MeV (HAL QCD)
  Lyu, Aoki, Doi, Hatsuda, Ikeda, Meng 2023
- $E_{\text{pole}} = -62 \pm 34$ MeV, **virtual state** at $m_\pi = 391$ MeV
  Whyte, Wilson, Thomas 2024

Introduction - Naming convention for poles

General naming convention for poles in the complex k-plane:

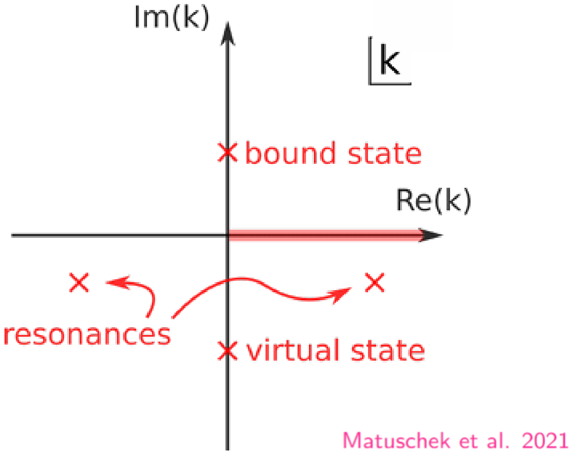

A comprehensive classification of poles in the energy plane can be found, e.g., in the review of hadronic molecules by Guo et al. 2022

Introduction - Motivation

Motivation for calculating observables as a function of pion mass:

- Studying analytic properties of the scattering amplitude and their impact on pole positions
- The nature of states can be probed using lattice simulations at unphysical quark masses Matuschek, Baru, Guo, Hanhart 2021
- Connecting different scenarios for T_{cc}^{+} at higher pion masses with the physical world
- Developing a framework which can be adjusted for similar studies

Pole trajectories

Pole trajectories – DD^* scattering from chiral EFT

Express all parameters in terms of $\xi \equiv m_\pi / m_\pi^{\mathrm{ph}}$ and vary the pion mass using chiral extrapolations within χ**EFT**.

Baru et al. 2013, Cleven et al. 2011, J Gasser, H Leutwyler 1984...

$$V = V^{(0)}_{\mathrm{OPE}} + V^{(0)}_{\mathrm{CT}} + V^{(2)}_{\mathrm{CT}} + \dots =$$

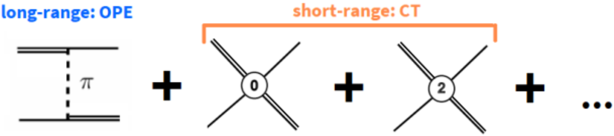

$$-\frac{g^2}{2f_\pi^2}\boldsymbol{\tau}_1 \cdot \boldsymbol{\tau}_2 (\epsilon_1 \cdot \boldsymbol{q})(\epsilon_2^* \cdot \boldsymbol{q}) D^\pi \qquad C^{(0)} \qquad C^{(2)}(p^2 + p'^2) + D^{(2)}(\xi^2 - 1)$$

$$m_{(*)} \to m_{(*)}(\xi),\ f_\pi \to f_\pi(\xi),\ g \to g(\xi)$$

$$V_{\mathrm{CT}} \to V_{\mathrm{CT}}(\xi)$$

$$T_{\alpha\beta} = V_{\alpha\gamma} - \sum_\beta \int \frac{\mathrm{d}^3 q}{(2\pi)^3} V_{\alpha\beta} G_\beta T_{\beta\gamma}$$

$\Rightarrow$ **Predict m_π-dependence of T_{cc}^+ observables by solving the LSE**

$\Rightarrow$ T_{cc}^+ **binding energy corresponds to poles in the DD^* scattering amplitude**

Pole trajectories - Closing phase space

By departing from physical point at $\xi = m_\pi / m_\pi^{\text{ph}} = 1$, the decay $D^* \to D\pi$ becomes kinematically forbidden already at $\xi_0 \approx 1.03$:

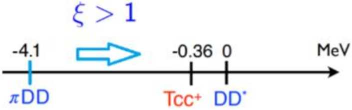

isospin limit

Dynamics of thresholds leads to **closing phase space**:

$\xi < 1.03$

$\xi \geq 1.03$

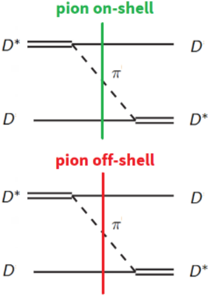

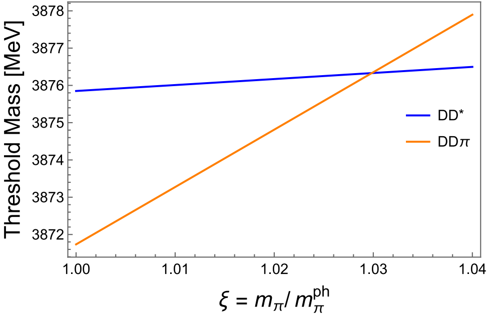

Crossing point: Two-body threshold coincides with three-body threshold at $\xi_0 \approx 1.03$

Pole trajectories - Closing phase space

$$\xi \equiv m_\pi / m_\pi^{\text{ph}}$$

Closing phase space $\Rightarrow$ T_{cc}^+ does a transition from quasi-bound to a fully bound state:

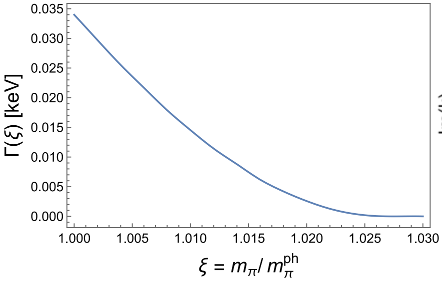

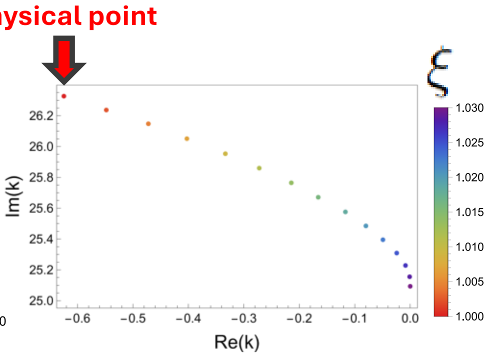

Decreasing full width Γ

LO pole trajectory in the complex k-plane

Pole trajectories - Character of poles

MA et al., 2407.04649v1 (2024)

$V = V_{\text{OPE}} + C_0$ → C_0 fixed at $E_{\text{pole}} = -0.36$ MeV for $\xi = 1$

Typical behavior of pole trajectories, demonstrated at LO:

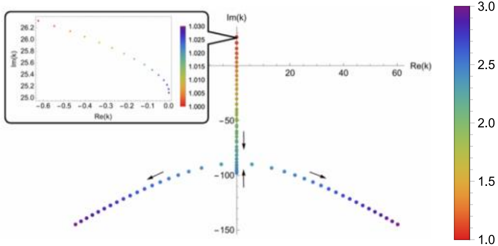

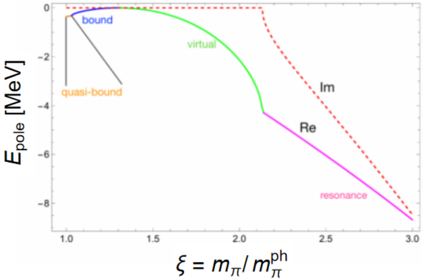

LO trajectory in **complex k-plane**
→ second virtual pole emerges from under the left-hand cut

LO trajectory for **energy**

Cusps ⇔ changing character of the pole

Pole trajectories - NLO trajectories

MA et al., 2407.04649v1 (2024)

$$V = V_{OPE} + C_0 + C_2(p^2 + p'^2) + D_2(\xi^2 - 1)$$

$\rightarrow C_2, D_2$ fixed from lattice phase shifts

NLO trajectories using input at $\xi \approx 2$ from the lattice data analysis of Meng et al. 2023 from lattice phase shifts by Padmanath, Prelovsek 2023:

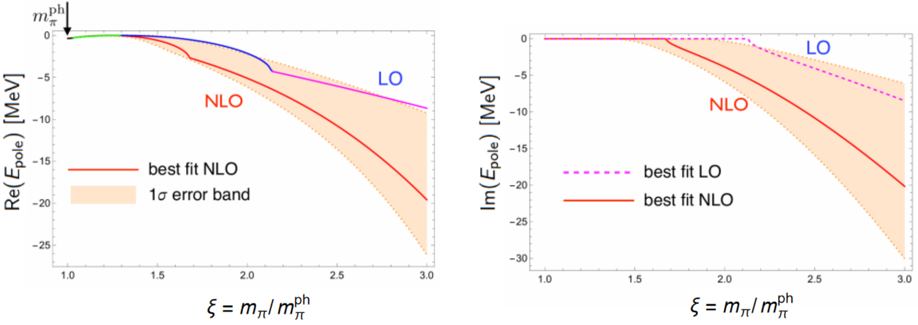

T_{cc}^+ pole transition: **quasi-bound** $\rightarrow$ **bound** $\rightarrow$ **virtual** $\rightarrow$ **resonance**

Pole trajectories - Pion vs pionless

MA et al., 2407.04649v1 (2024)

$$V = V_{OPE} + C_0 + C_2(p^2 + p'^2) + D_2(\xi^2 - 1)$$

$\rightarrow$ C_2, D_2 fixed from lattice phase shifts

The **pionless** pole trajectory is consistent with new lattice data at $m_\pi = 391$ MeV:

Whyte, Wilson, Thomas 2024

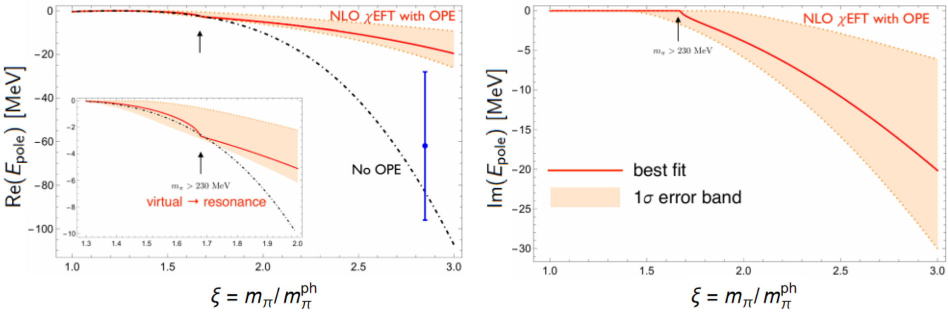

OPE plays a crucial role for the pole trajectory, especially regarding the formation of the T_{cc}^+ as a resonance state.

Pole trajectories - Summary and final remarks

- The pion mass dependence of the T_{cc}^{+} pole trajectory is investigated in chiral EFT
- Full analytic structure of the m_π dependent quantities is considered
- Chiral truncation errors are under control
- The cutoff dependence is small
- T_{cc}^{+} pole trajectory is

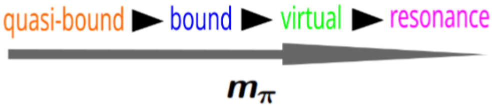

$\rightarrow$ consistent with the expectations from the **molecular picture**

Matuschek et al. 2021

- Serves as testable prediction for future lattice simulations

Backup

Backup - Chiral truncation errors & cutoff dependence

MA et al., 2407.04649v1 (2024)

Include higher-order contact terms to investigate chiral truncation errors:

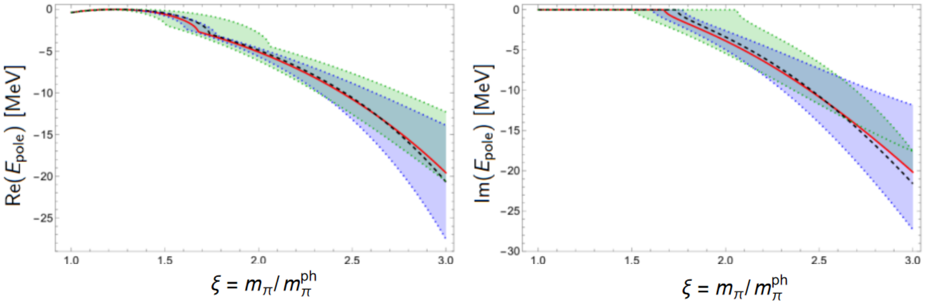

- Red solid curve: Best fit with $\Lambda = 700$ MeV
- **Black dashed curve**: Best fit with $\Lambda = 500$ MeV
- Green band: $\mathcal{O}(\xi^2, p^2)$ truncation uncertainty $V_{CT} \to V_{CT} + D_4(\xi^2 - 1)(p^2 + p'^2)$
- Blue band: $\mathcal{O}(\xi^4)$ truncation uncertainty $V_{CT} \to V_{CT} + \tilde{D}_4(\xi^4 - 1)$

Backup - Role of D-waves

$$V = V_{OPE} + C_0 + C_2(p^2 + p'^2) + D_2(\xi^2 - 1)$$

MA et al., 2407.04649v1 (2024)

NLO trajectories using input at $\xi \approx 2$ from the lattice data analysis of Meng et al. 2023 from lattice phase shifts by Padmanath, Prelovsek 2023:

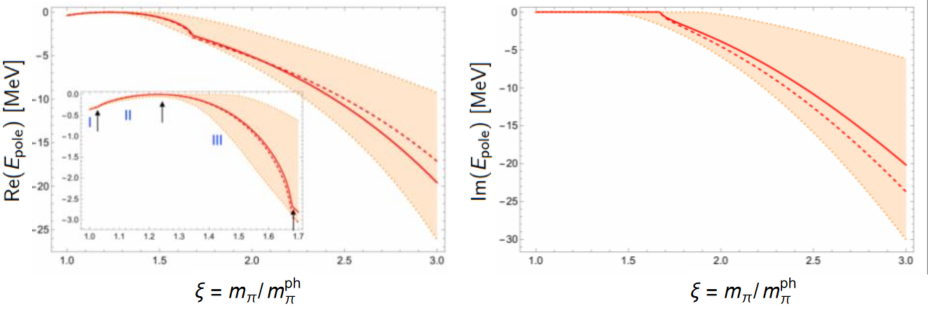

- Solid (dashed) red curve: S-wave (D-wave) OPE
- Orange band: statistical errors
- Regions I-III: quasi-bound, bound or virtual

Backup - Uncertainty for pionless trajectory

$$V = V_{OPE} + C_0 + C_2(p^2 + p'^2) + D_2(\xi^2 - 1)$$

$\rightarrow C_2, D_2$ fixed from lattice phase shifts

The **pionless** pole trajectory is consistent with new lattice data at $m_\pi = 391$ MeV: Whyte, Wilson, Thomas 2024

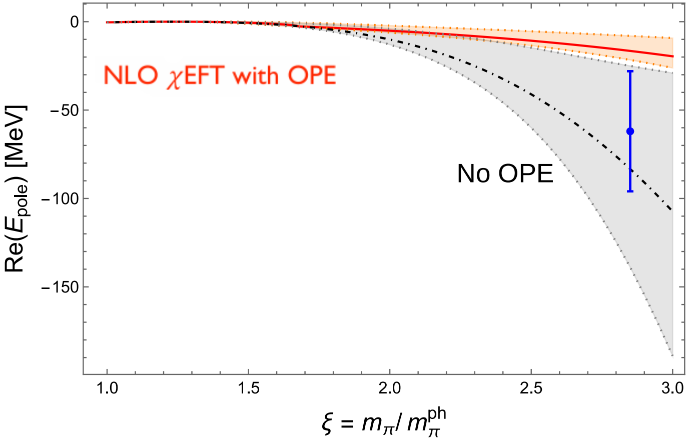

our error band for pionless case

Backup - DD^* scattering

$H_a = D_a + \boldsymbol{D}_a^* \cdot \boldsymbol{\sigma} \rightarrow$ superfields of light and heavy mesons

- The LO contact Lagrangian has the form

  Mehen and Powell 2011, AlFiky et al. 2006

$$\mathcal{L}_{HH} = -\frac{D_{00}}{8}\mathrm{Tr}(H_a^\dagger H_b H_b^\dagger H_a) - \frac{D_{01}}{8}\mathrm{Tr}(\sigma^i H_a^\dagger H_b \sigma^i H_b^\dagger H_a) \ldots$$

$\rightarrow D_{ij}$: low-energy constants describing contact interactions

- The LO Lagrangian for the $D^* D\pi$ interaction is given by

$$\mathcal{L} = \frac{1}{4} g \mathrm{Tr}(\sigma \cdot \mathbf{u}_{ab} H_b H_a^\dagger),$$

$$\boldsymbol{u} = -\frac{\nabla}{f_\pi}\begin{pmatrix} \pi^0 & \sqrt{2}\pi^+ \\ \sqrt{2}\pi^- & -\pi^0 \end{pmatrix}$$

Backup - DD^* scattering

Du, Baru, Dong, Filin, Guo, Hanhart, Nefediev, Nieves, Wang 2022

- The general one-pion exchange (OPE) potential is

$$V_{\rm OPE} = -\frac{g^2}{2f_\pi^2}\boldsymbol{\tau}_1 \cdot \boldsymbol{\tau}_2(\boldsymbol{\epsilon}_1 \cdot \boldsymbol{q})(\boldsymbol{\epsilon}_2^* \cdot \boldsymbol{q})D^\pi$$

- The propagator includes three-body effects: $M = m_{*c} + m_0 + E$

$$D^\pi = -\frac{1}{2\omega_\pi}\left(D_1^\pi + D_2^\pi\right),$$

$$D^\pi_{k\in\{1,2\}} = \left(m_i + m_j + \frac{p^2}{2m_i} + \frac{p'^2}{2m_j} + \overbrace{\omega_\pi(p, p', z)}^{\sqrt{m_\pi^2+(\boldsymbol{p}-\boldsymbol{p}')^2}} - M - i\epsilon\right)^{-1}$$

- Solve the LSE:

$$T_{\alpha\beta} = V_{\alpha\gamma} - \sum_\beta \int \frac{\mathrm{d}^3 q}{(2\pi)^3} V_{\alpha\beta} G_\beta T_{\beta\gamma}$$

Backup - NLO ansatz

$$\xi \equiv m_\pi / m_\pi^{\mathrm{ph}}$$

$$V_{\mathrm{CT}} = \underbrace{C_0 + D_2(\xi^2 - 1)}_{c_0(\xi)} + \underbrace{[C_2 + D_4(\xi^2 - 1)]}_{c_2(\xi)}(p^2 + p'^2)$$

The NLO contact ansatz has 4 parameters and the following constraints:

- $\xi = 1$, experimental data: fix C_0
  - $\rightarrow$ fit C_0 such that $\mathrm{Re}(E_B) = -0.36$ MeV
  - $\rightarrow$ set $D_4 \overset{!}{=} 0$
- $\xi_0 \approx 2$, lattice data: fix D_2 and C_2 based on analysis of Meng et al. 2023

$$V_{\mathrm{CT}}(p, p', \xi) = C_0 + D_2(\xi^2 - 1) + C_2(p^2 + p'^2)$$
$$D_2 = \frac{c_0(\xi_0) - C_0}{\xi_0^2 - 1},\ C_2 = c_2(\xi_0)$$